Inorganic Chemistry

Article

pubs.acs.org/IC

Origin of Magnetization Reversal and Exchange Bias Phenomena in Solid Solutions of $BiFeO_3$–$BiMnO_3$: Intrinsic or Extrinsic?

Alexei A. Belik*

International Center for Materials Nanoarchitectonics (WPI-MANA), National Institute for Materials Science, Namiki 1-1, Tsukuba, Ibaraki, 305-0044, Japan

Supporting Information

ABSTRACT: Magnetic properties of $BiFe_{0.7}Mn_{0.3}O_3$ (with a Néel temperature (T_N) of 425 K) and $BiFe_{0.6}Mn_{0.4}O_3$ (with T_N = 350 K) were investigated by magnetic measurements between 5 and 400 K. They crystallize in space group *Pnma* with the $\sqrt{2}a_p \times 4a_p \times 2\sqrt{2}a_p$ superstructure (a_p is the parameter of the cubic perovskite subcell) with a = 5.57800(9) Å, b = 15.7038(3) Å, and c = 11.22113(16) Å for $BiFe_{0.6}Mn_{0.4}O_3$. Both compounds show magnetization reversal or negative magnetization phenomena. However, it was found that the magnetization reversal is dependent on magnetic prehistory of a sample and measurement protocols. No magnetization reversal was observed when virgin samples were measured below T_N. Magnetization reversal effects appeared only when the samples were cooled in small magnetic fields from temperatures above T_N or after the samples were magnetized. The exchange bias effect or a shift of isothermal magnetization curves, depending on the measurement conditions, was also observed. The exchange bias changes its sign as a function of temperature and cooling conditions. Our findings allowed us to propose the extrinsic origin (related to sample inhomogeneities) of the magnetization reversal effect in these two compounds.

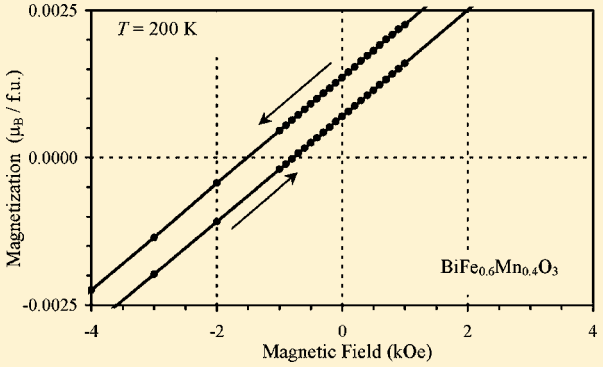

1. INTRODUCTION

$BiFeO_3$ and $BiMnO_3$ are two most-studied simple and single-phase multiferroics.[1,2] $BiFeO_3$ is both ferroelectric with the ferroelectric Curie temperature (T_E) of 1100 K and antiferromagnetic with the Néel temperature (T_N) of 640 K.[1] $BiMnO_3$ is the only true ferromagnetic material (with the ferromagnetic Curie temperature (T_C) of 100 K) among $BiMO_3$ (where M is a transition metal),[2] and it can possess ferroelectric properties in thin films.[3] The magnetism of $BiFeO_3$ and $BiMnO_3$ seems to be simple. However, low-temperature magnetic anomalies were observed in both $BiFeO_3$ and $BiMnO_3$ below T_N and T_C,[1,2,4−6] whose origin is still a matter of debate. In $BiFeO_3$, the spins are canted below T_N; however, because of the cycloidal rotation of the canted antiferromagnetic spins, the net moment is zero.

$(1 - x)BiFeO_3$–$xBiMnO_3$ solid solutions are formed for $0.0 \le x \le 0.3$ at ambient pressure, and the ambient-pressure $BiFe_{1-x}Mn_xO_{3+\delta}$ samples have *R*3*c* symmetry.[7−11] The $(1 - x)BiFeO_3$–$xBiMnO_3$ solid solutions can be stabilized in the entire composition range by the high-pressure synthesis method.[11,12] The high-pressure $BiFe_{1-x}Mn_xO_3$ samples have *R*3*c* symmetry for $0.0 \le x \le 0.1$, the *Pnma* symmetry with the $\sqrt{2}a_p \times 4a_p \times 2\sqrt{2}a_p$ superstructure (a_p is the parameter of the cubic perovskite subcell) for $0.1 \le x \le 0.6$, and the *C*2/*c* symmetry for $0.6 \le x \le 1$.[12] An interesting effect of magnetization reversal was recently found in the high-pressure $BiFe_{0.5}Mn_{0.5}O_3$ sample,[13] when the magnetization becomes negative or opposite to the applied magnetic field. This effect in $BiFe_{0.5}Mn_{0.5}O_3$ was explained by intrinsic properties as a result of a competition between single-ion magnetic anisotropy and Dzyaloshinsky–Moriya interactions.[13] Magnetization reversal was originally predicted and observed in some ferrimagnets having several magnetic sublattices, and the effect appears because of different temperature dependence of sublattice magnetizations.

Magnetization reversal effects were observed in other perovskite solid solutions, for example, in $YFe_{0.5}Cr_{0.5}O_3$,[14−16] and also in simple perovskites containing one transition metal, for example, in YVO_3.[17,18] The magnetization reversal was considered to be an intrinsic effect in YVO_3.[17] However, an alternative explanation (due to inhomogeneities caused by defects) was recently suggested.[18] Therefore, more work is needed to understand the magnetization reversal effect in perovskites.

In this work, we investigated magnetic properties of the high-pressure $BiFe_{0.7}Mn_{0.3}O_3$ and $BiFe_{0.6}Mn_{0.4}O_3$ samples. Under certain conditions, we observed the magnetization reversal effects in these compounds. However, it was found that the magnetization reversal is dependent on magnetic prehistory of a sample and measurement protocols. Magnetization reversal effects appeared only after the samples were magnetized by a

Received: October 31, 2012
Published: January 31, 2013

dx.doi.org/10.1021/ic302384j | *Inorg. Chem.* 2013, 52, 2015−2021

large magnetic field or when they were cooled in small magnetic fields from temperatures above T_N. Our finding allowed us to exclude "intrinsic" magnetic exchange interactions as the origin of the magnetization reversal in $BiFe_{0.7}Mn_{0.3}O_3$ and $BiFe_{0.6}Mn_{0.4}O_3$ and propose the "extrinsic" origin of the magnetization reversal related to sample inhomogeneities.

2. EXPERIMENTAL SECTION

$BiFe_{1-x}Mn_xO_3$ samples with x = 0.3, 0.4, 0.5, and 0.6 were synthesized from stoichiometric mixtures of Bi_2O_3 (99.9999%), Fe_2O_3 (99.999%), and Mn_2O_3 (99.99%) in a belt-type high-pressure apparatus at 6 GPa and 1400 K for 90 min in sealed gold capsules. After heat treatment, the samples were quenched to room temperature, and the pressure was slowly released.[11]

X-ray powder diffraction (XRPD) data were collected at room temperature on a Rigaku Ultima III diffractometer using Cu Kα radiation (2θ range of 7−110°, a step width of 0.02°, and a counting time of 2−12 s/step). All the samples contained traces of nonmagnetic $Bi_2O_2CO_3$ impurity (<1 wt %). $BiFe_{0.7}Mn_{0.3}O_3$ and $BiFe_{0.6}Mn_{0.4}O_3$ contained one perovskite-type phase with space group *Pnma* and the $\sqrt{2}a_p \times 4a_p \times 2\sqrt{2}a_p$ superstructure and the lattice parameters of a = 5.59412(10) Å, b = 15.6782(2) Å, and c = 11.24336(18) Å for $BiFe_{0.7}Mn_{0.3}O_3$ and a = 5.57800(9) Å, b = 15.7038(3) Å, and c = 11.22113(16) Å for $BiFe_{0.6}Mn_{0.4}O_3$. However, we found that $BiFe_{0.5}Mn_{0.5}O_3$ already contained several perovskite-type phases (probably three phases; see the Supporting Information). It should be mentioned that the second perovskite phase (~5 wt %) in addition to the main *Pnma* phase was also detected in $BiFe_{0.5}Mn_{0.5}O_3$ in ref 13. $BiFe_{0.4}Mn_{0.6}O_3$ contained a majority (~80 wt %) of the *C*2/*c* phase (observed in the $BiMnO_3$-rich side of the $BiFe_{1-x}Mn_xO_3$ system)[12] and ~20% of the *Pnma* phase. Therefore, only $BiFe_{0.7}Mn_{0.3}O_3$ and $BiFe_{0.6}Mn_{0.4}O_3$ (in the form of very loose pellets) were the subject of magnetic studies.

Magnetization measurements were performed on superconducting quantum interference device (SQUID) magnetometers (Quantum Design, MPMS 1 and 7 T) between 2 and 400 K in different applied fields under both zero-field-cooled (ZFC) conditions on warming (ZFCW) and field-cooled (FC) conditions on cooling (FCC). Between 2 and 400 K, samples could be measured continuously to low temperatures where the magnetization reversal takes place. In the ZFCW regime, a sample was rapidly (within 3−5 min) inserted into magnetometers, which were kept at 10 K. We also distinguish measurements on fresh or virgin samples (those measurements will be called v-ZFCW and v-FCC), which were not under the influence of any magnetic fields (except for the Earth's field).

We paid special attention on a trapped magnetic field inside magnetometers for ZFC measurements and measurements in low magnetic fields. Our Quantum Design MPMS instruments have the "reset magnet" option, where superconducting magnets are warmed. The "reset magnet" option reduces the absolute value of the trapped magnetic field below about 1 Oe. Then, we used an Nb superconducting sample and the iterative process to reduce (if needed) the trapped magnetic field below 0.1 Oe (at the sample position) and keep it positive. We reduced the absolute value of the magnetization (M) of a powder Nb sample (~100 mg) below 10^{-4} emu at 5 K, cf., M(Nb) = -1.32×10^{-2} emu at 10 Oe, M(Nb) = -6.52×10^{-2} emu at 50 Oe, and M(Nb) = -1.30×10^{-1} emu at 100 Oe. A negative trapped magnetic field could introduce some artifacts on ZFCW curves.[18,19]

Isothermal magnetization measurements were performed from 50 kOe to −50 kOe and from −50 kOe to 50 kOe at different temperatures (samples were cooled to the desired temperature at 50 kOe from 400 K with the cooling rate of 10 K/min). In a few cases, the ZFC isothermal magnetization measurements were performed (that is, a sample was quenched or cooled (at 10 K/min) in a zero magnetic field (more precisely, in a very small positive trapped magnetic field), and measurements were first performed from 0 to 50 kOe). Details are specified in the text for each measurement. Another measurement protocol is described in the Supporting Information (Table S1).

For $BiFe_{0.7}Mn_{0.3}O_3$, high-temperature magnetization measurements were performed using an oven attachment at 100 Oe. The first and second cycles were measured between 300 K and 540 K, and the third cycle between 300 K and 670 K.

Differential scanning calorimetry (DSC) curves were recorded on a Mettler Toledo DSC1 STAR^e system at a heating/cooling rate of 10 K/min under N_2 flow from 293 K to 420 K for $BiFe_{0.6}Mn_{0.4}O_3$ and from 293 K to 640 K for $BiFe_{0.7}Mn_{0.3}O_3$ in open Al capsules. DSC measurements were cycled three times to check the reproducibility of thermal effects. No significant differences were observed among three cycles. We note that, for both samples, DSC curves were also recorded up to 773 K, but no additional anomalies were observed.

3. RESULTS AND DISCUSSION

The DSC measurements showed weak anomalies near 350 K in $BiFe_{0.6}Mn_{0.4}O_3$ and 425 K in $BiFe_{0.7}Mn_{0.3}O_3$ (Figure 1).

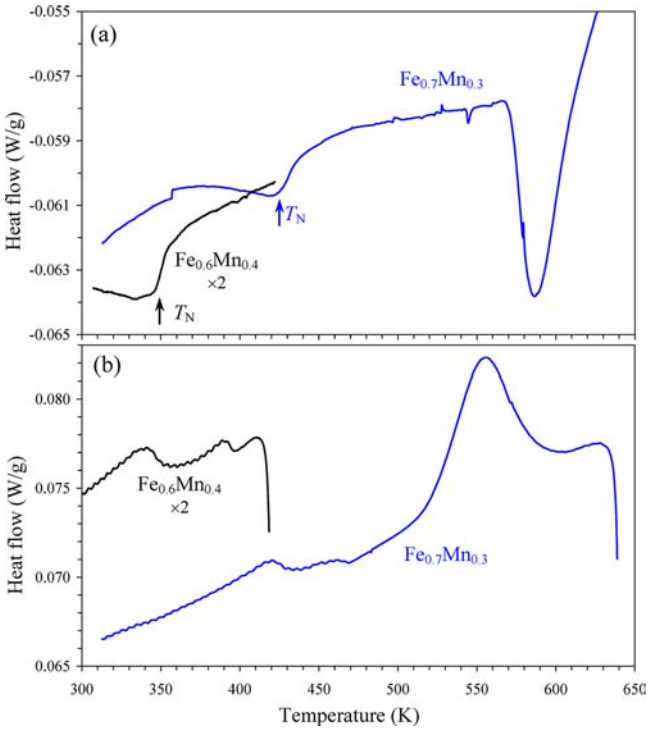

Figure 1. DSC curves (third runs) of $BiFe_{0.6}Mn_{0.4}O_3$ (black trace) and $BiFe_{0.7}Mn_{0.3}O_3$ (blue trace) upon (a) heating and (b) cooling. The DSC values for $BiFe_{0.6}Mn_{0.4}O_3$ were multiplied by 2. The arrows show the Néel temperatures (T_N). The small peak near 545 K in panel (a) originated from a metallic Bi impurity.

Magnetic measurements (see below) confirmed that these anomalies correspond to their Néel temperature (T_N). Within the magnetic measurement range of 2−400 K, we always stayed below T_N in $BiFe_{0.7}Mn_{0.3}O_3$ and could cross T_N in $BiFe_{0.6}Mn_{0.4}O_3$. There were much stronger reversible DSC anomalies near 590 K (on heating curves) and 550 K (on cooling curves) in $BiFe_{0.7}Mn_{0.3}O_3$; they probably correspond to a first-order structural phase transition.

Figure 2a shows v-ZFCW and v-FCC $\chi-T$ curves of $BiFe_{0.7}Mn_{0.3}O_3$ at 100 Oe. In this case, no magnetization reversal was observed. Figure 2b shows ZFCW and FCC curves of $BiFe_{0.7}Mn_{0.3}O_3$ at 100 Oe after measurements of the $M-H$ curves between −50 kOe to 50 kOe at 5 K and 300 K, that is, after the influence of a strong magnetic field. In this case, the magnetization reversal was detected at 60 K. The FCC curve was almost identical with the ZFCW curve; in other words,

dx.doi.org/10.1021/ic302384j | Inorg. Chem. 2013, 52, 2015−2021

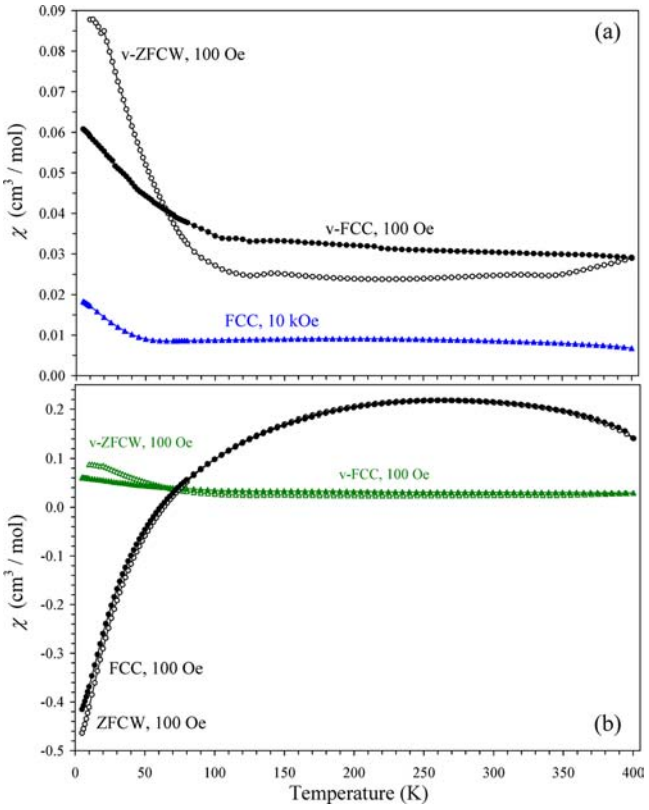

Figure 2. (a) v-ZFCW (white circles) and v-FCC (black circles) $\chi-T$ curves of the virgin $BiFe_{0.7}Mn_{0.3}O_3$ sample at 100 Oe and the FCC $\chi-T$ curve at 10 kOe (blue triangles). (b) ZFCW (white circles) and FCC (black circles) $\chi-T$ curves of $BiFe_{0.7}Mn_{0.3}O_3$ at 100 Oe after the sample was used for $M-H$ measurements at 5 and 300 K between −50 kOe to 50 kOe. The v-ZFCW and v-FCC $\chi-T$ curves from panel (a) are shown for comparison by green triangles.

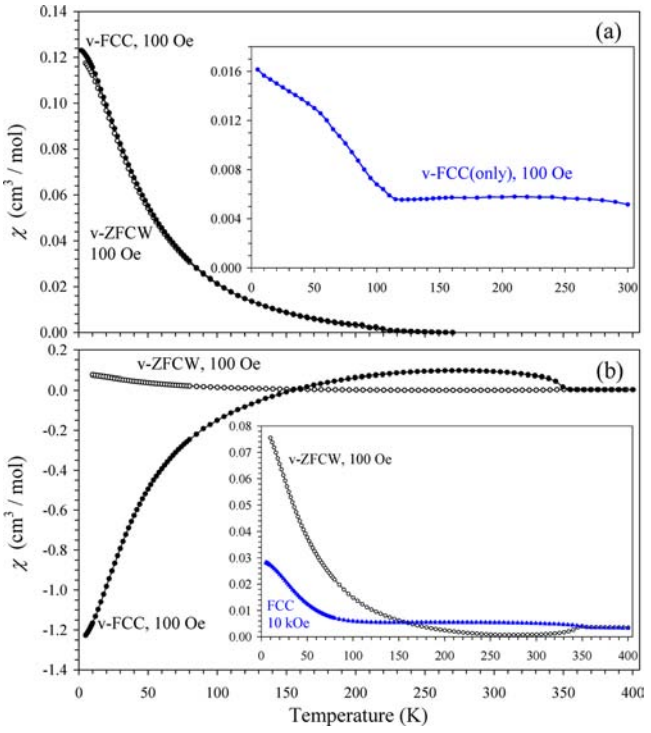

Figure 3. (a) v-ZFCW (white circles) and v-FCC (black circles) $\chi-T$ curves of the virgin $BiFe_{0.6}Mn_{0.4}O_3$ sample at 100 Oe between 5 and 270 K (below T_N). The insert gives the v-FCC(only) curve at 100 Oe (blue circles), that is, the virgin $BiFe_{0.6}Mn_{0.4}O_3$ sample was inserted into a magnetometer kept at 300 K (and having a very small positive trapped magnetic field), then a magnetic field of 100 Oe was applied, and the measurement was performed from 300 K to 5 K. (b) v-ZFCW (white circles) and v-FCC (black circles) $\chi-T$ curves of the virgin $BiFe_{0.6}Mn_{0.4}O_3$ sample at 100 Oe between 5 and 400 K (above T_N). The insert gives the same v-ZFCW curve at 100 Oe up to 400 K (white circles) and a FCC $\chi-T$ curve at 10 kOe (blue triangles).

there was a "memory" effect. The χ values (say, at 400 K) were strongly dependent on the applied magnetic field (see Figure 2a for 100 Oe and 10 kOe) and the magnetic prehistory of the sample (see Figure 2b). This behavior of the χ values is quite typical for materials having a (weak) ferromagnetic component and T_N (T_C) above the maximum measurement temperature. In other words, magnetic behavior is strongly dependent on the magnetic prehistory of a sample.

The main panel of Figure 3a shows v-ZFCW and v-FCC $\chi-T$ curves of $BiFe_{0.6}Mn_{0.4}O_3$ at 100 Oe when the measurement was performed below T_N (between 5 K and 270 K). In this case, no magnetization reversal was detected on the v-FCC curve, and the v-ZFCW and v-FCC curves were almost identical.

Figure 3b depicts v-ZFCW and v-FCC χ-T curves of $BiFe_{0.6}Mn_{0.4}O_3$ at 100 Oe when the measurement was performed above T_N (between 5 K and 400 K). In this case, the v-FCC curve demonstrated the magnetization reversal effect at ∼150 K. The magnetization reversal was observed on both ZFCW and FCC $\chi-T$ curves of $BiFe_{0.6}Mn_{0.4}O_3$ (at 100 Oe and when the measurement was performed below or above T_N) after the sample was used for different $M-H$ measurements between −50 kOe to 50 kOe (Figure 4). The "memory" effect on the ZFCW and FCC curves was again observed. The compensation temperature (where the magnetization is zero) decreased with increasing the measurement magnetic field in the FCC regime. The negative magnetization was still observed

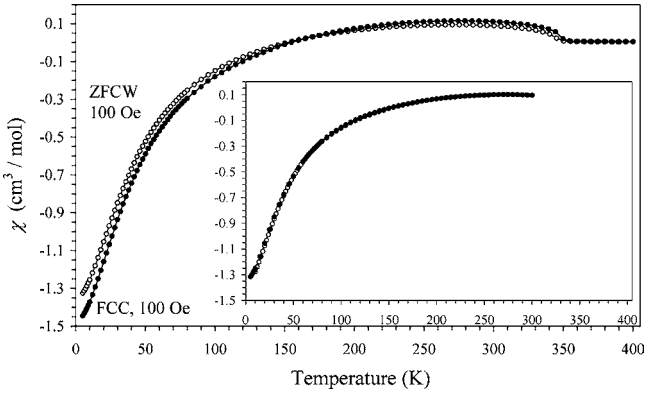

Figure 4. ZFCW (white circles) and FCC (black circles) $\chi-T$ curves of $BiFe_{0.6}Mn_{0.4}O_3$ at 100 Oe between 5 K and 400 K after the sample was used for different $M-H$ measurements between −50 kOe to 50 kOe. The insert gives ZFCW (white circles) and FCC (black circles) $\chi-T$ curves of magnetized $BiFe_{0.6}Mn_{0.4}O_3$ at 100 Oe between 5 K and 300 K (below T_N).

at 50 K under 4 kOe in $BiFe_{0.6}Mn_{0.4}O_3$, but no magnetization reversal was detected under 5 kOe (see the Supporting Information).

We also performed only v-FCC measurements from 300 K and from 400 K (they will be called v-FCC(only)), that is, the virgin $BiFe_{0.6}Mn_{0.4}O_3$ sample was inserted into a magnetometer

dx.doi.org/10.1021/ic302384j | Inorg. Chem. 2013, 52, 2015−2021

kept at 300 K (and having a very small positive trapped magnetic field), then a magnetic field of 100 Oe was applied at 300 K or 400 K (after increasing temperature from 300 K to 400 K), and the measurement was performed from 300 K to 5 K or from 400 K to 5 K. There was no magnetization reversal in the v-FCC(only) measurement from 300 K (the insert of Figure 3a). The v-FCC(only) curve from 400 K was almost identical to the v-FCC curve of Figure 3b (see the Supporting Information).

It should be mentioned that the magnetization was very small between 220 and 270 K on the main panel of Figure 3a for the v-ZFCW curve. On the other hand, the magnetization was larger and positive in the insert of Figure 3b during another similar measurement. In some cases, the magnetization on the v-ZFCW curves was negative, starting from ~180 K or 220 K up to ~345 K (see the Supporting Information). We could not fully understand reasons behind this behavior. It could be dependent on the fact that different parts of the virgin sample were used. The trapped magnetic field could also have an effect, considering the drastic effect of the trapped magnetic field on magnetization reversal in YVO_3.[18]

Figure 5 depicts isothermal magnetization curves of $BiFe_{0.6}Mn_{0.4}O_3$ and $BiFe_{0.7}Mn_{0.3}O_3$ at 5 and 300 K. The $M-H$ curves of $BiFe_{0.6}Mn_{0.4}O_3$ were investigated in details (Figures 6 and 7). No detectable hysteresis was observed at 400 K (above T_N), and the $M-H$ curve was linear (the R^2 value of the linear fit was 1). The $M-H$ curves of $BiFe_{0.6}Mn_{0.4}O_3$ changed from the S-type shape (at 5–30 K) to the elongated cigar-type shape (at 100 and 300 K). It is interesting that no detectable hysteresis was observed at the intermediate temperature of 150 K (Figure 7b), where the magnetization reversal takes place, and the $M-H$ curve was linear (the R^2 value of the linear fit was 1).

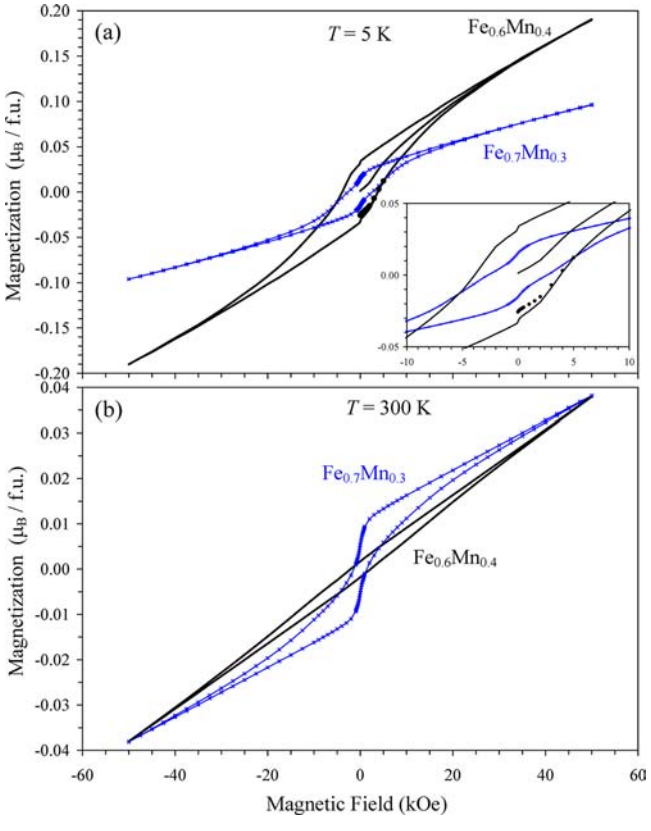

Figure 5. (a) $M-H$ curves of $BiFe_{0.7}Mn_{0.3}O_3$ and $BiFe_{0.6}Mn_{0.4}O_3$ at 5 K. The insert gives details near the origin. Black lines show the $M-H$ curves of the virgin $BiFe_{0.6}Mn_{0.4}O_3$ sample in the ZFC mode (starting from a zero magnetic field). Black dots show the initial ZFC $M-H$ curve (starting from a zero magnetic field) of the magnetized $BiFe_{0.6}Mn_{0.4}O_3$ sample. (b) $M-H$ curves of $BiFe_{0.7}Mn_{0.3}O_3$ and $BiFe_{0.6}Mn_{0.4}O_3$ at 300 K.

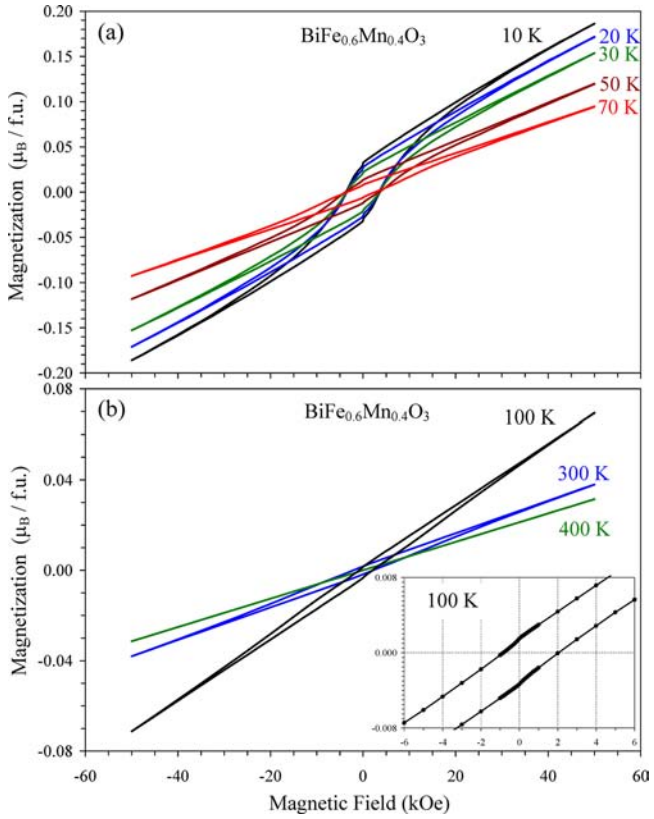

Figure 6. $M-H$ curves of $BiFe_{0.6}Mn_{0.4}O_3$ at different temperatures: (a) at 10, 20, 30, 50, and 70 K (see the Supporting Information for the measurement protocol) and (b) at 100, 300, and 400 K. The inset gives details near the origin at 100 K.

As can be seen from Figure 6b (the inset) and Figure 7, shifts of the $M-H$ curves were observed or asymmetric behavior relative to the origin. These are indications of the so-called exchange bias (EB) effects.[20] Shifts of $M-H$ curves can be characterized by (1) the exchange bias field, H_{EB}, defined as $H_{EB} = (H_+ + H_-)/2$, where H_+ and H_- are the coercive field on the positive (right) and negative (left) sides of the $M-H$ curves, respectively; (2) the remanent asymmetry, M_{EB}, defined as $M_{EB} = (M_+ + M_-)/2$, where M_+ and M_- are the positive (up) and negative (down) remanent magnetization, respectively; and (3) the saturation asymmetry, S_{EB}, defined as $S_{EB} = (S_+ + S_-)/2$, where S_+ and S_- are magnetization at the maximum and minimum field, respectively.[20] We note that H_+ and H_- were determined by the linear extrapolation between two points where the magnetization changes the sign. Different parameters of the $M-H$ curves under different cooling conditions are summarized in Table 1 and in the Supporting Information. The temperature dependence of H_{EB}, M_{EB}, and S_{EB} is shown in Figure 8. The exchange bias field and the remanent asymmetry change their signs near 150 K. This behavior is called the tunable exchange bias.

Some time ago, it was believed that positive exchange bias ($H_{EB} > 0$) and tunable exchange bias effects are rather rare.[20]

dx.doi.org/10.1021/ic302384j | Inorg. Chem. 2013, 52, 2015–2021

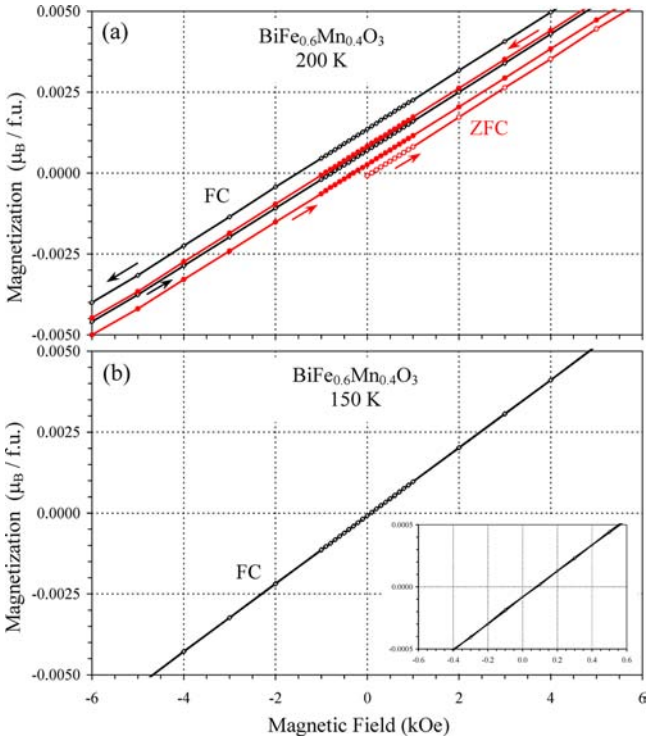

Figure 7. (a) $M-H$ curves of $BiFe_{0.6}Mn_{0.4}O_3$ at 200 K in the ZFC mode (cooled in 0 Oe from 400 K) (red circles) and in the FC mode (cooled in 50 kOe from 400 K) (gray diamonds). (b) $M-H$ curves of $BiFe_{0.6}Mn_{0.4}O_3$ at 150 K in the FC mode (cooled in 50 kOe from 400 K). The insert gives details near the origin.

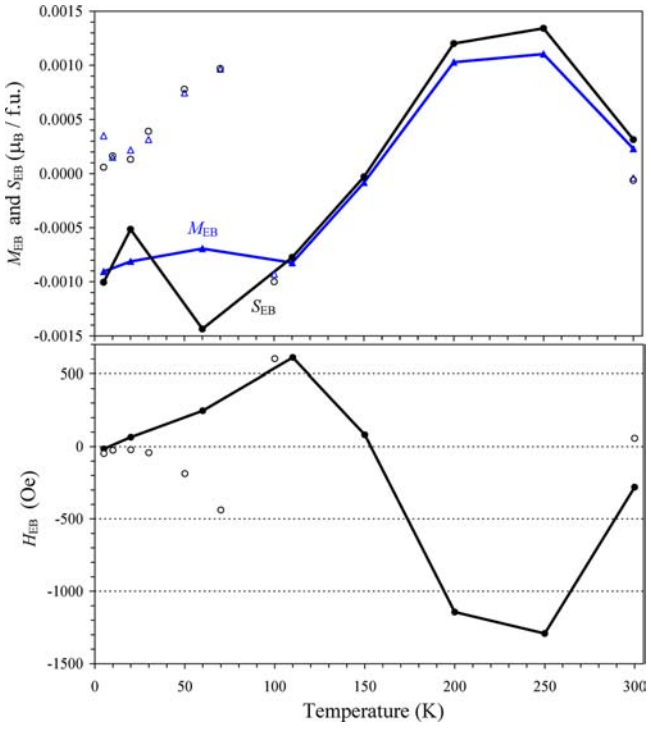

Figure 8. Temperature dependence of (a) the remanent asymmetry (M_{EB}) and the saturation asymmetry (S_{EB}) and (b) the exchange bias field (H_{EB}) in $BiFe_{0.6}Mn_{0.4}O_3$ under the FC conditions at 50 kOe from 400 K (filled symbols). White symbols show the M_{EB}, S_{EB}, and H_{EB} values for a different measurement protocol (see the Supporting Information (Table S1) for details of the protocol).

However, tunable exchange bias, as a function of temperature or the value of the initial cooling field, has recently been observed in many perovskite-type systems with canted antiferromagnetism that show the magnetization reversal phenomenon.[14,15,21−23] Therefore, tunable exchange bias and magnetization reversal phenomena are closely related, and the tunable exchange bias seems to be a primary effect. The exchange bias phenomenon is attributed to ferromagnetic (FM)−antiferromagnetic (AFM) interfaces, when the anisotropy is induced in the FM part when the system is cooled through the Néel temperature of the AFM part under an applied magnetic field and under the condition that T_N of the AFM part is smaller than T_C of the FM part.[20] The exchange bias effect has been observed in core−shell nanoparticles, phase-separated bulk materials, and in many multilayered thin films.[20] In other words, the exchange bias effect requires interfaces or inhomogeneities.

We indeed observed that the magnetization reversal effect occurs only when the virgin $BiFe_{0.6}Mn_{0.4}O_3$ sample is cooled through T_N (Figure 3b). If the effect were intrinsic (that is, caused by a competition between different (Fe−Fe, Fe−Mn, and Mn−Mn) Dzyaloshinsky−Moriya interactions and by

Table 1. Exchange Bias Parameters of the $M-H$ Curves for $BiFe_{0.6}Mn_{0.4}O_3$ under Different Conditions

T (K)	S_+ (μ_B)	S_- (μ_B)	$S_{EB} \times 10^4$ (μ_B)	$M_+ \times 10^4$ (μ_B)	$M_- \times 10^4$ (μ_B)	$M_{EB} \times 10^4$ (μ_B)	H_+ (Oe)	H_- (Oe)	H_{EB} (Oe)
ZFC from 300 K (rapidly inserted within 3−5 min to 10 K)									
5	0.1904	−0.1903	0.578	330.968	−323.977	3.495	3807	−3905	−49
FC at 100 Oe from 400 K (after the FCC measurement at 100 Oe from 400 K to 5 K)									
5	0.1882	−0.1886	−1.947	326.532	−338.213	−5.841	3564	−3409	77
ZFC from 400 K (with 10 K/min)									
200	0.0448	−0.0437	5.867	8.306	2.616	5.461	−303	−928	−616
FC at 50 kOe from 400 K (with 10 K/min)									
5	0.1863	−0.1883	−10.037	343.743	−361.855	−9.056	3519	−3553	−17
20	0.1700	−0.1711	−5.149	265.263	−281.513	−8.125	3254	−3126	64
60	0.1071	−0.1100	−14.355	85.554	−99.426	−6.936	3518	−3025	247
110	0.0649	−0.0664	−7.737	9.383	−25.862	−8.239	1912	−691	611
150	0.0521	−0.0522	−0.298	−0.821	−0.818	−0.819	78	83	81
200	0.0456	−0.0432	12.019	13.595	6.993	10.294	−773	−1514	−1144
250	0.0424	−0.0397	13.417	20.475	1.619	11.047	−182	−2402	−1292
300	0.0397	−0.0391	3.146	20.505	−15.924	2.291	1876	−2438	−281
400	0.0315	−0.0314	0.253	0.045	−0.015	0.015			

dx.doi.org/10.1021/ic302384j | Inorg. Chem. 2013, 52, 2015−2021

single-ion magnetic anisotropy), it should be observable during measurements below T_N and would not require cooling through T_N in small magnetic fields. Tunable exchange bias is also demonstrated in Figures 7 and 8.

Magnetic susceptibilities should be independent of a magnetic field above T_N or T_C, that is, in a paramagnetic region. Figure 9 shows the inverse magnetic susceptibilities

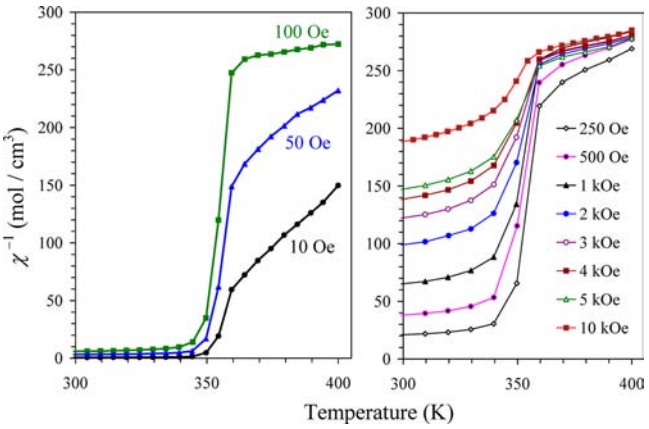

Figure 9. Inverse magnetic susceptibilities $((1/\chi)-T)$ of $BiFe_{0.6}Mn_{0.4}O_3$ in the FCC mode at different magnetic fields. The data from 400 K to 300 K are shown.

$((1/\chi)-T)$ of $BiFe_{0.6}Mn_{0.4}O_3$ at different magnetic fields. They were quite different at small magnetic fields of 10, 50, and 100 Oe. Approximate (because of the limited temperature range of 370−400 K) estimations of the effective magnetic moment gave $4.69\mu_B$ at 100 Oe and only $1.94\mu_B$ at 10 Oe. We emphasize that we performed the "reset magnet" procedure before measurements at each (small) magnetic field, and the deviation of the real magnetic field from the nominal field cannot account for such large difference in the χ^{-1} values. In addition, we saw no noticeable difference in the χ^{-1} values (say, at 10 and 100 Oe) for paramagnetic materials measured with our magnetometers. Therefore, Figure 9 is a clear indication of the presence of a ferromagnetic-like "impurity" with T_C above 400 K. This ferromagnetic-like "impurity" may consist, in general, of a real magnetic impurity (which exists as a separate phase in a very small amount undetectable by XRPD) or may be a result of clustering effects. By clustering effects, we mean iron-enriched $BiFe_{0.6+x}Mn_{0.4-x}O_3$ regions. These regions should have higher magnetic transition temperatures and weak ferromagnetism and could serve as a FM part in FM−AFM interfaces. We emphasize that the analysis of the $(1/\chi)-T$ plots above T_N at different magnetic fields is a very simple and sensitive tool to detect the presence of "ferromagnetic-like impurities" (of course, under the condition that the real magnetic field is carefully controlled at small values). However, to the best of our knowledge, this analysis has never been reported in papers related to the magnetization reversal phenomena in perovskite-type systems with canted antiferromagnetism.

Figure 10 shows the inverse magnetic susceptibilities for $BiFe_{0.7}Mn_{0.3}O_3$ between 300 and 670 K measured at 100 Oe. The first (and second) cycles were performed between 300 and 540 K. These data confirmed that T_N of $BiFe_{0.7}Mn_{0.3}O_3$ is ~425 K. The difference between heating and cooling curves starts from the maximum measurement temperature of 540 K. This is an indication of the presence of a "ferromagnetic-like" component with a higher transition temperature. The measure-

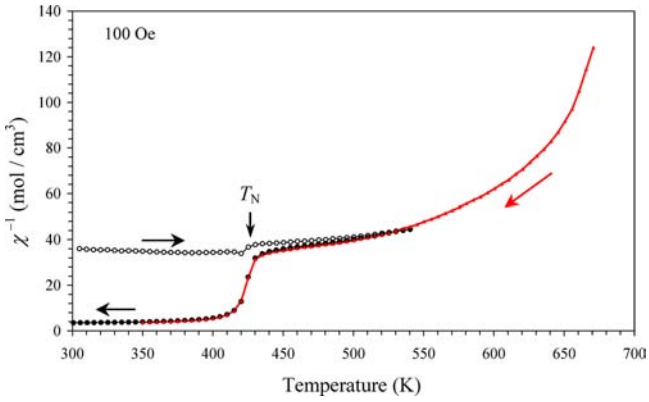

Figure 10. Inverse magnetic susceptibilities $((1/\chi)-T)$ of virgin $BiFe_{0.7}Mn_{0.3}O_3$ at 100 Oe. The sample was first heated from 300 K to 540 K (white circles) and then cooled from 540 K to 300 K (black circles); then, the second cycle between 300 K and 540 K was performed (not shown). In the third cycle, the sample was heated from 300 K to 670 K (not shown) and cooled from 670 K to 350 K (red triangles). The arrows show heating−cooling directions.

ment up to 670 K showed the absence of Curie−Weiss behavior and sharp increase of the inverse susceptibilities near 650 K. This is another indication of the presence of a "ferromagnetic-like" component. We note that the behavior cannot be caused by possible (partial) sample decomposition, because XRPD measurements showed no change in the XRPD pattern after high-temperature magnetization measurements, in comparison with the XRPD pattern of the as-synthesized sample. $BiFe_{0.7}Mn_{0.3}O_3$ was also stable up to 773 K in the DSC experiment (see the Supporting Information).

Therefore, we demonstrated the existence of the FM part with T_C above T_N in the canted AFM $BiFe_{0.6}Mn_{0.4}O_3$ and $BiFe_{0.7}Mn_{0.3}O_3$ systems, and there exists a basis for the appearance of exchange bias. Of course, single-ion magnetic anisotropy and Dzyaloshinsky−Moriya interactions play their roles in the formation of canted AFM states. However, the tunable exchange bias effect and the magnetization reversal effect, as a result, are caused by "extrinsic" reasons, such as the presence of magnetic impurities (a real extrinsic origin) or sample inhomogeneities or even surface effects (a pseudo-extrinsic origin). The formation of trace amounts of magnetic impurities is quite possible, especially in systems containing two transition metals (e.g., Fe−Mn, Fe−Cr, and Mn−Cr). It should also be mentioned that intrinsic magnetic phase separation occurs in doped manganites, and the magnetic separation is the origin of the colossal magnetoresistance effect. The exchange bias effect was observed in phase-separated manganites because of the existence of small FM domains within the AFM host.[24] A surface transition was recently detected in bulk $BiFeO_3$.[25] This is why we used above the term "pseudo-extrinsic", because sample inhomogeneity and phase separation (if exist) and surface effects are difficult to avoid or eliminate.

When the samples were magnetized, the FM "impurity" creates an effective negative field on the main phase, resulting in negative magnetization. The magnetic behavior of the entire system may be dependent on the temperature dependence of magnetization in the FM "impurity" explaining the "memory" effect or the overlap of the ZFCW and FCC curves (see Figures 2b and 4).

Exchange bias effects have recently been observed in thin films of classical multiferroic $BiFeO_3$. Using magnetic force

dx.doi.org/10.1021/ic302384j | Inorg. Chem. 2013, 52, 2015−2021

microscopy measurements, it was demonstrated that the exchange bias effects are "extrinsic" and caused by the presence of a ferrimagnetic/ferromagnetic material at the grain boundaries of AFM $BiFeO_3$ forming a core−shell structure.[26] Exchange bias effects were observed in the ambient-pressure $BiFe_{0.8}Mn_{0.2}O_3$ nanoparticles, because of their core−shell structure.[27] Negative magnetization was observed in the ambient-pressure $BiFe_{0.75}Mn_{0.25}O_3$ pellets.[11] However, the effect disappeared just by grinding pellets into powder.[11] These examples and our current results show that the interpretation of magnetization reversal effects is a difficult task and should be done with care and requires much experimental data.

In summary, we demonstrated that the magnetization reversal effect in $BiFe_{0.7}Mn_{0.3}O_3$ and $BiFe_{0.6}Mn_{0.4}O_3$ is dependent on magnetic prehistory of the samples and measurement protocols. No magnetization reversal was observed when the virgin samples were measured below T_N. Magnetization reversal effects appeared only after the samples were magnetized or when they were cooled in small magnetic fields from temperatures above T_N. We also observed the tunable exchange bias effect and the existence of ferromagnetic-like "impurities" above T_N. Our results allowed us to suggest the "extrinsic" origin (related to sample inhomogeneities) of magnetization reversal in $BiFe_{0.7}Mn_{0.3}O_3$ and $BiFe_{0.6}Mn_{0.4}O_3$. Our conclusion is consistent with the recent findings for YVO_3.[18] We hope that our results will stimulate further detailed experimental and theoretical work and discussion on the origin of magnetization reversal in perovskite materials.

■ ASSOCIATED CONTENT

Supporting Information

Full content of ref 25, XRD patterns of $BiFe_{0.6}Mn_{0.4}O_3$, $BiFe_{0.5}Mn_{0.5}O_3$, and $BiFe_{0.7}Mn_{0.3}O_3$ (after the DSC experiment up to 773 K); the FCC curve at 10 Oe, the $M-H$ curve at 250 K, the v-FCC(only) curve from 400 K, the inverse magnetic susceptibilities, and parameters of the $M-H$ curves of $BiFe_{0.6}Mn_{0.4}O_3$. This information is available free of charge via the Internet at http://pubs.acs.org.

■ AUTHOR INFORMATION

Corresponding Author

*E-mail: Alexei.Belik@nims.go.jp.

Notes

The authors declare no competing financial interest.

■ ACKNOWLEDGMENTS

This work was supported by World Premier International Research Center Initiative (WPI Initiative, MEXT, Japan), the NIMS Individual-Type Competitive Research Grant, the Japan Society for the Promotion of Science (JSPS) through its "Funding Program for World-Leading Innovative R&D on Science and Technology (FIRST Program)", and the Grants-in-Aid for Scientific Research (No. 22246083) from JSPS, Japan.

■ REFERENCES

(1) Catalan, G.; Scott, J. F. *Adv. Mater.* **2009**, *21*, 2463.
(2) Belik, A. A. *J. Solid State Chem.* **2012**, *195*, 32.
(3) Jeen, H. J.; Singh-Bhalla, G.; Mickel, P. R.; Voigt, K.; Morien, C.; Tongay, S.; Hebard, A. F.; Biswas, A. *J. Appl. Phys.* **2011**, *109*, 074104.
(4) (a) Singh, M. K.; Prellier, W.; Singh, M. P.; Katiyar, R. S.; Scott, J. F. *Phys. Rev. B* **2008**, *77*, 144403. (b) Singh, M. K.; Katiyar, R. S.; Prellier, W.; Scott, J. F. *J. Phys.: Condens. Matter* **2009**, *21*, 042202.
(5) Belik, A. A.; Takayama-Muromachi, E. *Inorg. Chem.* **2006**, *45*, 10224.
(6) Belik, A. A.; Takayama-Muromachi, E. *J. Phys.: Condens. Matter* **2008**, *20*, 025211.
(7) Sosnowska, I.; Schäfer, W.; Kockelmann, W.; Andersen, K. H.; Troyanchuk, I. O. *Appl. Phys. A: Mater. Sci. Process* **2002**, *74*, S1040.
(8) Yang, C.-H.; Koo, T. Y.; Jeong, Y. H. *Solid State Commun.* **2005**, *134*, 299.
(9) Selbach, S. M.; Tybell, T.; Einarsrud, M. A.; Grande, T. *Chem. Mater.* **2009**, *21*, 5176.
(10) Selbach, S. M.; Tybell, T.; Einarsrud, M. A.; Grande, T. *Phys. Rev. B* **2009**, *79*, 214113.
(11) Belik, A. A.; Abakumov, A. M.; Tsirlin, A. A.; Hadermann, J.; Kim, J.; Van Tendeloo, G.; Takayama-Muromachi, E. *Chem. Mater.* **2011**, *23*, 4505.
(12) Azuma, M.; Kanda, H.; Belik, A. A.; Shimakawa, Y.; Takano, M. *J. Magn. Magn. Mater.* **2007**, *310*, 1177.
(13) Mandal, P.; Sundaresan, A.; Rao, C. N. R.; Iyo, A.; Shirage, P. M.; Tanaka, Y.; Simon, C.; Pralong, V.; Lebedev, O. I.; Caignaert, V.; Raveau, B. *Phys. Rev. B* **2010**, *82*, 100416.
(14) Mao, J. H.; Sui, Y.; Zhang, X. Q.; Wang, X. J.; Su, Y. T.; Liu, Z. G.; Wang, Y.; Zhu, R. B.; Wang, Y.; Liu, W. F.; Liu, X. Y. *Solid State Commun.* **2011**, *151*, 1982.
(15) Mao, J. H.; Sui, Y.; Zhang, X. Q.; Su, Y. T.; Wang, X. J.; Liu, Z. G.; Wang, Y.; Zhu, R. B.; Wang, Y.; Liu, W. F.; Tang, J. K. *Appl. Phys. Lett.* **2011**, *98*, 192510.
(16) Dasari, N.; Mandal, P.; Sundaresan, A.; Vidhyadhiraja, N. S. *Europhys. Lett.* **2012**, *99*, 17008.
(17) (a) Ren, Y.; Palstra, T. T. M.; Khomskii, D. I.; Nugroho, A. A.; Menovsky, A. A.; Sawatzky, G. A. *Phys. Rev. B* **2000**, *62*, 6577. (b) Ren, Y.; Palstra, T. T. M.; Khomskii, D. I.; Pellegrin, E.; Nugroho, A. A.; Menovsky, A. A.; Sawatzky, G. A. *Nature* **1998**, *396*, 441.
(18) Tung, L. D.; Lees, M. R.; Balakrishnan, G.; McK. Paul, D. *Phys. Rev. B* **2007**, *75*, 104404.
(19) Kumar, N.; Sundaresan, A. *Solid State Commun.* **2010**, *150*, 1162.
(20) Nogues, J.; Schuller, I. K. *J. Magn. Magn. Mater.* **1999**, *192*, 203.
(21) Yoshii, K. *Appl. Phys. Lett.* **2011**, *99*, 142501.
(22) Singh, R. P.; Tomy, C. V.; Grover, A. K. *Appl. Phys. Lett.* **2010**, *97*, 182505.
(23) Manna, P. K.; Yusuf, S. M.; Shukla, R.; Tyagi, A. K. *Appl. Phys. Lett.* **2010**, *96*, 242508.
(24) Niebieskikwiat, D.; Salamon, M. B. *Phys. Rev. B* **2005**, *72*, 174422.
(25) Jarrier, R.; et al. *Phys. Rev. B* **2012**, *85*, 184104.
(26) Sung, K. D.; Park, Y. A.; Seo, M. S.; Jo, Y.; Hur, N.; Jung, J. H. *J. Appl. Phys.* **2012**, *112*, 033915.
(27) Manna, P. K.; Yusuf, S. M.; Shukla, R.; Tyagi, A. K. *Phys. Rev. B* **2011**, *83*, 184412.